Brilliance
Research of Artificial Intelligence

E-ISSN : 2807-9035
Volume 6, **Number** 4, November 2026
https://doi.org/10.47709/brilliance.v6i4.9992

Priority-Based Self-Healing for LTE QoS Using User Density and Traffic Load

Fidyatun Nisa[1*], Arnawan Hasibuan[2], Nanda Sitti Nurfebruary[3]
[1,3]Department of Information Systems, Universitas Malikussaleh, Lhokseumawe, Indonesia; [2]Department of Electrical Engineering, Universitas Malikussaleh, Lhokseumawe, Indonesia
[1*]fidyatun.nisa@unimal.ac.id, [2]arnawan@unimal.ac.id, [3]nandasitti.nur@unimal.ac.id

open access

***Corresponding Author**

Article History:
Submitted: 08-11-2026
Accepted: 18-11-2026
Published: 23-11-2026

Keywords:
AHP; LTE; QoS; self-healing; traffic load; user density.

Brilliance: Research of Artificial Intelligence is licensed under a Creative Commons Attribution-NonCommercial 4.0 International (CC BY-NC 4.0).

ABSTRACT

LTE self-healing commonly prioritizes radio or capacity conditions, while spatial user concentration and traffic demand are less explicitly integrated into recovery ordering. Objective: This study develops a priority-based self-healing model combining user density, estimated traffic load, and radio-quality degradation for LTE recovery. Methods: Population and spatial data covering 68 gampong in Lhokseumawe Municipality were integrated with secondary LTE measurements from eight locations. User Density Index (Di), Traffic Load Index (Ti), and QoS Degradation Index (Qi) were normalized to [0,1]. Analytic Hierarchy Process (AHP) was applied to obtain criterion weights, and the Priority Recovery Score (PRS) was implemented in Python. Multi-cell overload scenarios were evaluated using conventional and PRS-based recovery. Results: Density ranged from 672 to 8,700 inhabitants/km². AHP weights were 0.1638 for Di, 0.2973 for Ti, and 0.5390 for Qi, with a consistency ratio of 0.79%. The highest PRS was 0.624 at Alue Awe, followed by 0.608 at Kuta Blang. After source-destination accounting was corrected, three multi-cell scenarios with initial overloads of 1,668, 3,150, and 3,306 users reached zero remaining overload and 100% simulated recovery in 3, 5, and 5 cycles. Maximum utilization decreased to 100%, and maximum Network Risk Proxy decreased from 0.979 to 0.954 in Scenario 1 and from 1.008 to 0.954 in Scenarios 2 and 3. Conclusion: The model provides a proof of concept for location-aware recovery prioritization. PRS changed recovery order but did not improve final recovery rate or final risk relative to conventional recovery in the tested scenarios.

INTRODUCTION

Long Term Evolution (LTE) remains an important mobile broadband technology, but the increasing number of connected users and spatially uneven demand make network management more difficult. A failure or severe degradation in one serving cell can redistribute users to neighboring cells and increase the load of already active cells. Self-healing is therefore an important function within Self-Organizing Networks (SON), where abnormal conditions are detected and compensated through automated or semi-automated actions. Recent research has increasingly connected self-healing with machine learning, anomaly detection, network analytics, and zero-touch management (Zhang et al., 2022; Sangaiah et al., 2022; El Rajab et al., 2024).

Earlier LTE research established cell outage compensation as a way to mitigate coverage, capacity, and service-quality degradation after cell failures. More recent approaches have introduced learning-based detection, simulation-based compensation, and coordinated healing. Omar et al. (2021a) developed a self-healing simulator for 5G small cells, while Omar et al. (2021b) proposed a self-healing model using precoding and big-data processing. Oğuz and Kalaycıoğlu (2022) demonstrated the use of LSTM and one-dimensional CNN for cellular anomaly detection, and Sangaiah et al. (2022) emphasized automated fault detection and diagnosis as key elements of intelligent network management.

Another research direction considers traffic behavior. Mobile traffic is spatially and temporally dynamic, and a concentration of traffic in one cell may produce imbalance among adjacent cells. Haider et al. (2023) investigated network-load prediction and anomaly detection, Rao et al. (2023) modeled dynamic spatial and temporal correlations in cellular traffic, and Gu et al. (2023) proposed a city-level spatial-temporal transformer for cellular traffic prediction. Li et al. (2024) further showed that traffic-peak prediction is closely related to the detection of traffic imbalance between adjacent cells. These studies support the importance of traffic demand as contextual information for network management.

Radio quality remains another essential dimension. RSRP, RSRQ, and SNR provide information about received signal strength, signal quality, and the relationship between useful signal and interference/noise. QoS-aware resource allocation studies have shown that service performance is affected by changing radio conditions and resource availability (Mai & Hu, 2022; Ortega & Tralli, 2022). Recent LTE QoS assessment has also demonstrated the value of combining multiple indicators into a composite quality measure (Zaldivar-Herrera et al., 2024). In self-healing research,

This is an Creative Commons License This work is licensed under a Creative Commons Attribution-NonCommercial 4.0 International License.

Brilliance
Research of Artificial Intelligence

E-ISSN : 2807-9035
Volume 6, **Number** 4, November 2026
https://doi.org/10.47709/brilliance.v6i4.9992

spatial information is increasingly relevant: Mata et al. (2024) used spatial graphs to support performance-degradation root-cause analysis, while Bayazeed et al. (2024) investigated location-aware coordination of multiple self-healing instances.

In Lhokseumawe Municipality, population density is spatially heterogeneous. Official statistics provide population and density information at village and subdistrict levels (BPS-Statistics Lhokseumawe Municipality, 2025). Welfare statistics report that 69.47% of the population aged five years and over accessed the Internet in 2023 (BPS-Statistics Lhokseumawe Municipality, 2024); in this study, this value is used only as a transparent proxy for potential Internet users, not as LTE subscriber counts or operator traffic. The research gap addressed here is the integration of spatial user concentration, estimated traffic demand, and radio-quality degradation into a single and interpretable recovery-priority mechanism for LTE.

The objective of this study is to develop a Priority Recovery Score (PRS) that combines User Density Index (Di), Traffic Load Index (Ti), and QoS Degradation Index (Qi), and to evaluate its role in self-healing recovery ordering. The contribution is a lightweight, location-aware decision layer that can prioritize recovery actions before a more complex compensation or artificial-intelligence controller is applied. The study also explicitly tests whether PRS produces better final recovery outcomes than a conventional ordering strategy, rather than assuming superiority.

LITERATURE REVIEW

This study therefore extends the authors' previous LTE self-healing research by introducing a Priority Recovery Score (PRS) as a decision layer for recovery prioritization. The proposed model integrates the User Density Index (D_i), Traffic Load Index (T_i), and QoS Degradation Index (Q_i). User density represents the potential spatial impact of a fault, traffic load represents relative service demand, and radio-quality degradation represents the severity of network-condition deterioration. The three indicators are normalized and combined using weights obtained through the Analytic Hierarchy Process (AHP). The resulting PRS is used to determine the order in which overloaded locations are processed by the self-healing mechanism. Thus, the contribution of this study is not another complex machine-learning detector, but a lightweight, location-aware, and interpretable decision layer that can complement conventional or more advanced self-healing controllers.

The reviewed studies indicate three major directions in current cellular self-healing research: intelligent fault detection and diagnosis, traffic-aware network analysis, and spatially aware network management. However, there remains a practical gap in combining the potential spatial impact of a fault, the relative service demand of an area, and the severity of radio degradation into a single, transparent recovery-priority mechanism. This gap is particularly relevant when operator traffic counters and active-user data are unavailable.

Radio and service-quality information remain important complementary dimensions. RSRP, RSRQ, and SNR provide measurable information about received signal strength and radio conditions and can therefore be used as indicators of network-quality degradation when complete end-user QoS measurements are unavailable. Ortega and Tralli (2022) demonstrated the importance of QoS-aware resource allocation in wireless networks, while Zaldivar-Herrera et al. (2024) showed that multiple LTE quality indicators can be combined into a composite QoS assessment. In the present study, these indicators are used specifically to construct a radio-quality degradation index rather than being interpreted as direct measurements of throughput, latency, jitter, or packet loss.

Recent work has further moved toward zero-touch and adaptive network automation. El Rajab et al. (2024) discussed zero-touch networks as a framework for integrating network observation, analysis, decision-making, and automated actions, while Caleb et al. (2025) investigated adaptive approaches for fault detection in self-healing networks. Such approaches illustrate the long-term direction toward increasingly autonomous cellular-network management. Nevertheless, highly intelligent approaches can require extensive training data, computational resources, and operator-grade network counters, which may not always be available in medium-sized urban areas or in research environments using secondary network data.

Spatial awareness has also become increasingly relevant to self-healing. Mata et al. (2024) proposed the use of spatial graphs for performance-degradation root-cause analysis toward self-healing mobile networks, demonstrating that spatial relationships among network elements can provide useful context for identifying degradation sources. Bayazeed et al. (2024) investigated location-aware coordination among multiple self-healing instances. These studies support the importance of spatial context, but spatial information is mainly used for root-cause analysis or coordination rather than being explicitly combined with user density and traffic load to determine recovery priority.

Traffic-aware network management provides another important research direction. Haider et al. (2023) investigated network-load prediction and anomaly detection using ensemble learning in 5G cellular networks. Rao et al. (2023) developed a deep-learning method for cellular traffic prediction that considers dynamic spatial and temporal correlations, while Gu et al. (2023) studied city-level cellular traffic using a spatial-temporal transformer. Li et al. (2024) further addressed prediction of traffic peaks in mobile networks. These studies demonstrate that traffic demand contains valuable spatial-temporal information; however, traffic prediction is generally not formulated as a direct recovery-priority mechanism for simultaneous network overload or cell-fault conditions.

Subsequent research has expanded self-healing toward data-driven and intelligent network management. Zhang

This is an Creative Commons License This work is licensed under a Creative Commons Attribution-NonCommercial 4.0 International License.

Brilliance
Research of Artificial Intelligence

E-ISSN : 2807-9035
Volume 6, **Number** 4, November 2026
https://doi.org/10.47709/brilliance.v6i4.9992

et al. (2022) reviewed data-driven machine-learning techniques for cellular self-healing and identified challenges involving data availability, real-time processing, and multi-source data integration. Oğuz and Kalaycıoğlu (2022) investigated LSTM and 1D-CNN approaches for anomaly detection in multi-tiered cellular networks, while Sangaiah et al. (2022) addressed automatic fault detection and diagnosis in cellular and beyond-5G networks. These studies demonstrate a transition from conventional fault management toward intelligent fault detection and diagnosis, but their primary objective remains identifying or classifying abnormal network conditions rather than ranking recovery urgency across affected locations.

Self-healing in cellular networks can be viewed as a closed-loop process involving fault detection, diagnosis, compensation, and recovery. The concept is closely associated with Self-Organizing Networks (SON) and is increasingly linked to automated network management.

Although recent studies have increasingly addressed QoS-aware, traffic-aware, and intelligent self-healing mechanisms, the integration of spatial user density, traffic load, and radio-quality degradation into a unified recovery-priority mechanism remains limited. The authors' earlier work on LTE fault management and self-healing (Nisa & Haryadi, 2016) provides the initial foundation for the present research direction. Building on this foundation and recent developments in self-healing networks, this study proposes a Priority Recovery Score (PRS) that combines user density, traffic load, and radio-quality degradation to determine location-aware recovery priorities in LTE networks.

METHOD

Research Design and Data

This study applies a quantitative model-development approach. The study area is Lhokseumawe Municipality, Aceh, Indonesia, and the object is LTE network condition viewed through spatial population concentration, estimated traffic demand, radio quality, and self-healing recovery. The final dataset combines population and spatial information for 68 gampong with secondary LTE measurements from eight observation locations. The spatial layer was processed in QGIS to classify population density. The LTE dataset contains RSRP, RSRQ, and SNR. Throughput, latency/delay, jitter, and packet loss were not available and were therefore not fabricated or treated as measured variables.

The eight observation locations were Alue Awe, Meunasah Manyang, Cut Mamplam, Buket Rata, Meunasah Mee, Blang Crum, Kuta Blang, and Keude Cunda. Buket Rata was represented by Mesjid Punteuet in the population dataset because that administrative unit was available for spatial matching. Population density was used as a spatial proxy for user concentration. The percentage 69.47% was applied to population to estimate potential Internet users. Because this factor is constant across locations, it does not alter min-max normalized traffic-load values; it only scales the absolute estimated-user values.

Table 1. LTE Observation Locations and Radio Measurements

Location	Density	RSRP (dBm)	RSRQ (dB)	SNR (dB)
Alue Awe	672	−100	−14	−2.0
Meunasah Manyang	737	−92	−12	−0.5
Cut Mamplam	739	−86	−15	−3.0
Buket Rata	820	−82	−11	10.0
Meunasah Mee	1,107	−85	−13	0.5
Blang Crum	1,440	−81	−10	9.0
Kuta Blang	5,894	−81	−13	3.0
Keude Cunda	8,700	−85	−12	−0.7

Table 1 summarizes the eight LTE observation locations used in the analysis. The density column represents the population-density value assigned to each observation point, while RSRP, RSRQ, and SNR describe the corresponding radio conditions. These measurements provide the empirical input for constructing the User Density Index (D_i) and the radio-quality component of Q_i. The density values span 672–8,700 inhabitants/km², providing spatial variation for the subsequent normalization and recovery-priority analysis.

Index Construction

The User Density Index is calculated using min-max normalization so that the location with the lowest observed density receives 0 and the highest receives 1:

$$D_i = (\text{Density}_i - \text{Density}_{min}) / (\text{Density}_{max} - \text{Density}_{min}) \quad (1)$$

Potential Internet users are estimated from population using the 69.47% proxy. The resulting value is normalized to obtain the Traffic Load Index:

$$U_i = P_i \times 0.6947 \quad (2)$$

$$T_i = (U_i - U_{min}) / (U_{max} - U_{min}) \quad (3)$$

This is an Creative Commons License This work is licensed under a Creative Commons Attribution-NonCommercial 4.0 International License.

Brilliance
Research of Artificial Intelligence

E-ISSN : 2807-9035
Volume 6, **Number** 4, November 2026
https://doi.org/10.47709/brilliance.v6i4.9992

Because only radio-quality variables were available, Qi is operationalized as a radio-quality degradation index. Each parameter is oriented so that a larger normalized value indicates worse relative condition, and the three components are averaged:

$$Q_i = (QRSRP_{,i} + QRSRQ_{,i} + QSNR_{,i}) / 3 \quad (4)$$

This operational definition is deliberately distinguished from complete end-user QoS. It is a model indicator derived from RSRP, RSRQ, and SNR and does not replace direct throughput, latency, jitter, or packet-loss measurements.

AHP and Priority Recovery Score

AHP was applied to the three criteria: user density (D), traffic load (T), and QoS degradation (Q). The pairwise matrix used in the model was [[1, 1/2, 1/3], [2, 1, 1/2], [3, 2, 1]]. The resulting weights were 0.1638, 0.2973, and 0.5390, respectively. The consistency ratio was 0.79%, below the commonly accepted 10% threshold. The weights should be interpreted as model assumptions rather than as empirical expert-survey estimates.

$$PRS_i = 0.1638D_i + 0.2973T_i + 0.5390Q_i \quad (5)$$

The PRS is used as a priority-ordering mechanism. A higher PRS means that the corresponding location is processed earlier when multiple cells require recovery. The score itself is not a recovery-rate metric; recovery performance is evaluated separately.

Self-Healing Simulation and Evaluation

The model was implemented in Python and developed through versions V1–V9. The development sequence included basic recovery, traffic-load variation, radio-degradation integration, neighbor-capacity constraints, conventional-versus-PRS comparison, multi-cell fault testing, risk evaluation, source-destination correction, and final evaluation. V10 was then added to clarify changes in maximum utilization and Network Risk Proxy after recovery. The simulation assumes a capacity of 4,000 users per cell and a maximum transfer of 1,000 users per recovery action. These are modeling parameters, not operator capacity values.

Three recovery strategies were compared: no self-healing as a baseline, conventional self-healing based on overload/capacity conditions, and PRS-based self-healing using the combined priority score. The main evaluation metrics were initial overload, remaining overload, recovery rate, recovery cycles, transferred users, maximum utilization, and a Network Risk Proxy. The risk proxy was defined as the average of the normalized radio-degradation index and utilization. The model was evaluated under single-cell traffic surges and three multi-cell overload scenarios.

The simulation was treated as a proof-of-concept validation. No claim was made that the simulated utilization or risk changes represent measured improvement in an operational LTE network.

RESULT

Spatial Distribution and Radio Conditions

The population dataset contains 68 gampong with a total population of 198,705 people. QGIS processing produced three populated-density classes used to describe spatial variation. The three highest-density gampong were Pusong Baru (21,789 inhabitants/km²), Pusong Lhokseumawe (13,502 inhabitants/km²), and Kampung Jawa Lhokseumawe (12,022 inhabitants/km²), all within Banda Sakti. The eight LTE observation points were selected to represent different density and radio conditions.

Figure 1 illustrates the spatial distribution of population density across Lhokseumawe City, mapped using QGIS based on village-level population data. The map shows considerable spatial variation in population density across the study area. Higher-density areas are mainly concentrated in the northern and central parts of the city, particularly within Banda Sakti District, whereas most areas of Blang Mangat, Muara Dua, and Muara Satu Districts are characterized by relatively lower population density.

This is an Creative Commons License This work is licensed under a Creative Commons Attribution-NonCommercial 4.0 International License.

Brilliance
Research of Artificial Intelligence
E-ISSN : 2807-9035
Volume 6, Number 4, November 2026
https://doi.org/10.47709/brilliance.v6i4.9992

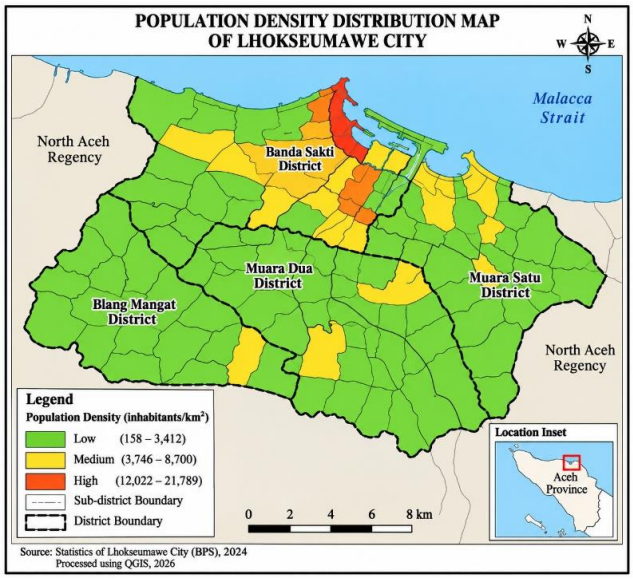


Figure 1. Population Density Distribution Map of Lhokseumawe City

The population density was classified into three categories: low (158–3,412 inhabitants/km²), medium (3,746–8,700 inhabitants/km²), and high (12,022–21,789 inhabitants/km²). The spatial pattern indicates that population distribution is not uniform across Lhokseumawe City, with high-density areas concentrated in specific urban locations. This spatial variation provides an important basis for identifying areas that may potentially experience greater service impact when a network disturbance occurs.

In this study, population density is used as a proxy for user concentration and is subsequently normalized to form the User Density Index (D_i). The index represents the relative concentration of potential users among the observation areas. However, population density is not used as the sole basis for recovery decisions. It is integrated with the Traffic Load Index (T_i) and the Radio Quality Degradation Index (Q_i) to formulate the Priority Recovery Score (PRS). Therefore, the spatial information presented in Figure 1 provides the geographical basis for incorporating user-related impact into the proposed LTE self-healing mechanism.

Proposed Self-Healing Framework

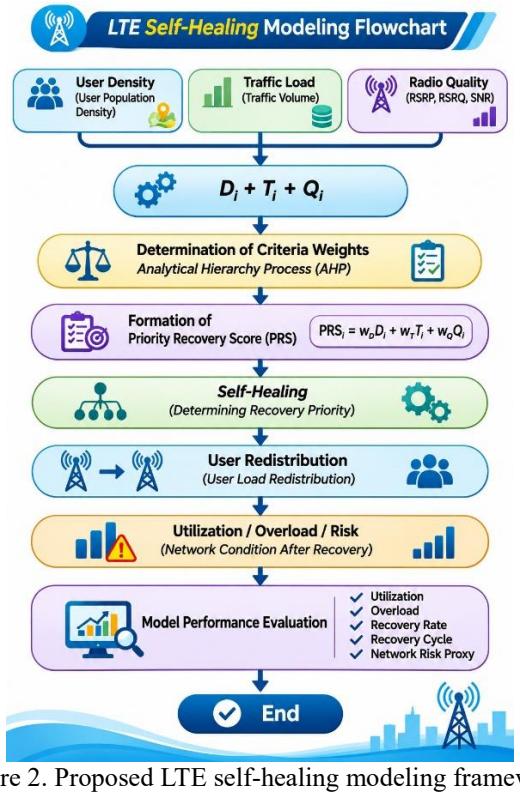


Figure 2. Proposed LTE self-healing modeling framework

This is an Creative Commons License This work is licensed under a Creative Commons Attribution-NonCommercial 4.0 International License.

Brilliance
Research of Artificial Intelligence
E-ISSN : 2807-9035
Volume 6, Number 4, November 2026
https://doi.org/10.47709/brilliance.v6i4.9992

Figure 2 presents the proposed LTE self-healing modeling framework. The model integrates user density, traffic load, and radio quality through the normalized indices (D_i), (T_i), and (Q_i). These indicators are weighted using the Analytical Hierarchy Process (AHP) and combined into the Priority Recovery Score (PRS), which determines the recovery priority. The self-healing mechanism then redistributes user loads to available neighboring capacity, after which network utilization, overload, and risk are evaluated. Model performance is assessed using utilization, overload, recovery rate, recovery cycles, and the network risk proxy.

Normalized Indices and Priority Recovery Score

The normalized values of the three criteria and the resulting Priority Recovery Score (PRS) for the eight observation locations are presented in Table 2. The User Density Index ((D_i)), Traffic Load Index ((T_i)), and QoS Degradation Index ((Q_i)) are normalized to the range of 0–1 and subsequently combined using the AHP-derived weights to obtain the PRS for each location. The table provides the quantitative basis for determining the relative recovery priority among the observation locations.

Table 2. Normalized Indices and Priority Recovery Score

Location	D_i	T_i	Q_i	PRS
Alue Awe	0.000	0.453	0.908	0.624
Meunasah Manyang	0.008	0.000	0.596	0.323
Cut Mamplam	0.008	0.240	0.754	0.479
Buket Rata	0.018	0.536	0.084	0.208
Meunasah Mee	0.052	0.371	0.514	0.396
Blang Crum	0.096	0.500	0.026	0.178
Kuta Blang	0.648	1.000	0.379	0.608
Keude Cunda	1.000	0.094	0.478	0.450

The results in Table 2 show that the PRS values vary across locations because the three criteria do not have identical spatial patterns. Alue Awe obtains the highest PRS (0.624), despite having the lowest (D_i), because of its relatively high (Q_i) and moderate (T_i). Kuta Blang has the second-highest PRS (0.608), supported by its high density and traffic indices. In contrast, Blang Crum has a relatively low PRS (0.178) because its radio-quality degradation index is low. These results demonstrate that the proposed PRS does not prioritize locations based on population density alone, but combines user concentration, traffic demand, and radio-quality degradation into a single recovery-priority measure.

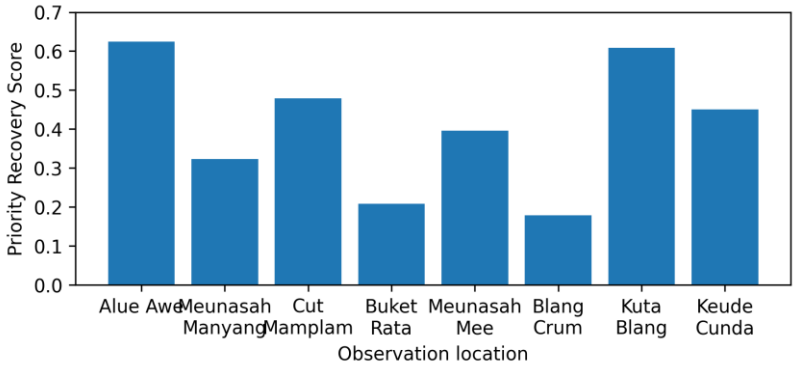


Figure 3. Priority Recovery Score across the eight LTE observation locations.

Figure 3 shows the PRS values obtained for the eight observation locations. Alue Awe has the highest PRS (0.624), followed by Kuta Blang (0.608), Cut Mamplam (0.479), Keude Cunda (0.450), Meunasah Mee (0.396), Meunasah Manyang (0.323), Buket Rata (0.208), and Blang Crum (0.178). The variation indicates that recovery priority is determined jointly by user density, traffic load, and radio-quality degradation rather than by density alone.

The normalized values demonstrate the multi-dimensional nature of the proposed score. D_i ranges from 0.000 to 1.000, T_i from 0.000 to 1.000, and Q_i from 0.026 to 0.908. Alue Awe receives the highest PRS of 0.624 even though its D_i is 0.000, because its Q_i is the highest and its traffic index is moderate. Kuta Blang ranks second at 0.608 because it combines high density, the highest traffic index, and moderate radio degradation. Keude Cunda has the maximum density index but a lower PRS of 0.450 because its traffic index is only 0.094.

This is an Creative Commons License This work is licensed under a Creative Commons Attribution-NonCommercial 4.0 International License.

Brilliance
Research of Artificial Intelligence

E-ISSN : 2807-9035
Volume 6, **Number** 4, November 2026
https://doi.org/10.47709/brilliance.v6i4.9992

Table 3. AHP Weights and Consistency

Criterion	Weight	Role
User Density (D_i)	0.1638	Spatial impact indicator
Traffic Load (T_i)	0.2973	Service-demand indicator
QoS Degradation (Q_i)	0.5390	Radio-condition indicator
Consistency Ratio	0.79%	Consistent matrix

Table 3 shows the relative contribution of the three criteria to the recovery-priority decision. QoS degradation (Q_i) receives the largest weight (0.5390), followed by the traffic load (T_i = 0.2973) and user density (D_i = 0.1638). The consistency ratio is 0.79%, indicating that the adopted pairwise comparison matrix is consistent under the model assumption. These weights are therefore used to calculate the PRS for each observation location.

Simulation Results

The 2.0× traffic surge in V2 produced overload at Alue Awe (104.95%), Buket Rata (113.90%), Blang Crum (110.00%), and Kuta Blang (163.80%). Cut Mamplam reached 82.15% load and Meunasah Mee 96.15%. V4 introduced neighbor-capacity constraints and showed that not every overloaded condition could be fully compensated. For example, Alue Awe under an extreme condition recovered 77.78% of 198 overloaded users, while Kuta Blang under an extreme condition recovered 58.54% of 2,552 overloaded users.

To examine whether the proposed PRS changes the recovery outcome, the conventional and PRS-based approaches were compared under five single-cell overload conditions, as summarized in Table 4.

Table 4. Conventional and PRS-based recovery in V5

Scenario	Overload	Conventional	PRS-based
Alue Awe Extreme	198	77.78%	77.78%
Buket Rata Extreme	556	100%	100%
Blang Crum Extreme	400	100%	100%
Kuta Blang Medium	914	100%	100%
Kuta Blang Extreme	2,552	58.54%	58.54%
Average	—	87.26%	87.26%

The V5 comparison shows that PRS did not improve the final recovery rate relative to conventional recovery in the tested single-cell scenarios. The average recovery rate was 87.26% for both approaches. This result is important because it prevents an unsupported claim that PRS itself increases recovery percentage.

V6 extended the evaluation to simultaneous multi-cell overload. In Scenario 1, conventional recovery started with Kuta Blang, whereas PRS-based recovery started with Alue Awe. Thus, the two methods produced different recovery orders even when the final recovery outcome was identical. V7 initially produced an increase in the risk indicator because transferred users were added to destination cells without being subtracted from source cells. This was identified as a state-accounting error rather than a network effect. V8 corrected the source-destination redistribution rule.

After correction, V9 reached zero remaining overload and 100% simulated recovery in all three multi-cell scenarios. Initial overloads were 1,668, 3,150, and 3,306 users, requiring 3, 5, and 5 recovery cycles, respectively. V10 further showed that maximum utilization decreased from 122.85% to 100% in Scenario 1 and from 163.80% to 100% in Scenarios 2 and 3. A final QoS-oriented proxy evaluation (V10) was then performed using maximum cell utilization before and after recovery. Across the three multi-cell scenarios, the maximum utilization decreased from 123% to 100% in Scenario 1 and from 163% to 100% in Scenarios 2 and 3 after recovery. Because utilization is used as a network-condition proxy, these results indicate reduction of simulated overload rather than a direct measurement of end-user throughput, latency, jitter, or packet loss.

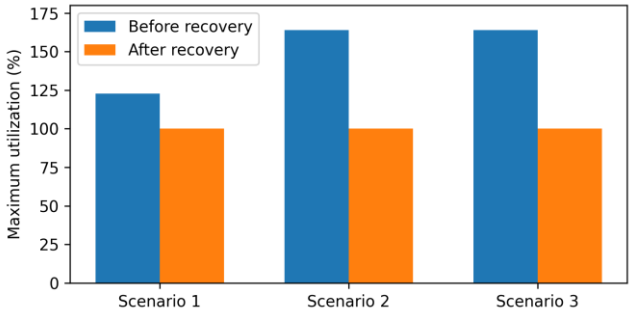


Figure 4. Maximum utilization before and after simulated recovery in the three multi-cell scenarios.

This is an Creative Commons License This work is licensed under a Creative Commons Attribution-NonCommercial 4.0 International License.

Brilliance
Research of Artificial Intelligence

E-ISSN : 2807-9035
Volume 6, **Number** 4, November 2026
https://doi.org/10.47709/brilliance.v6i4.9992

The maximum Network Risk Proxy also decreased after recovery. Scenario 1 declined from 0.979 to 0.954, while Scenarios 2 and 3 declined from 1.008 to 0.954. These changes represent improvements under the assumed simulation model and should not be interpreted as direct measurements of end-user QoS.

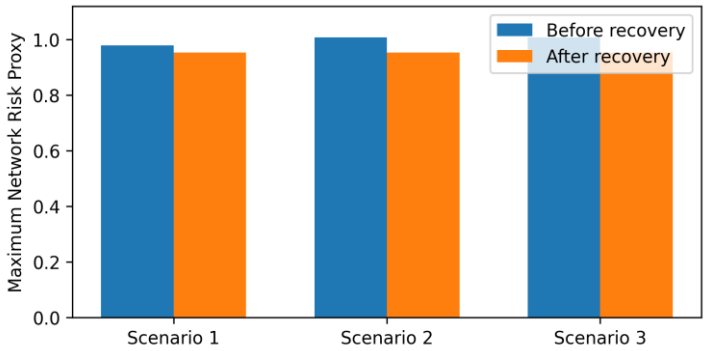


Figure 5. Maximum Network Risk Proxy before and after simulated recovery.

DISCUSSION

The first research question concerns the relationship among user density, traffic load, and LTE quality. The results show that the three dimensions vary independently enough that a single indicator is insufficient for recovery prioritization. The clearest example is Alue Awe, which has the lowest observed density but the highest radio-degradation index. Conversely, Keude Cunda has the highest density but only a moderate degradation index and a low traffic index. Therefore, high population concentration does not automatically imply the highest recovery urgency. This is consistent with the broader direction of mobile-network management research, where traffic behavior, radio conditions, and spatial context are increasingly treated as complementary information rather than interchangeable KPIs (Rao et al., 2023; Li et al., 2024; Mata et al., 2024).

The AHP weights provide an interpretable representation of this multi-criteria decision. Radio degradation receives the largest weight (0.5390), followed by traffic load (0.2973) and user density (0.1638). Under the current model assumptions, this means that a severe radio-quality problem can dominate the recovery priority even when population density is low. The result is not a universal weighting for LTE networks; it is a reproducible weighting configuration for this proof-of-concept model. Future studies should replace the assumed pairwise matrix with expert judgments, operator policies, or data-driven weight optimization.

The second research question concerns the formulation of self-healing using user density and traffic load as recovery-priority information. The PRS fulfills this role by converting three normalized dimensions into a single ordering variable. This differs from compensation methods that directly modify antenna parameters, power allocation, or user association. Instead, PRS functions as a decision layer that determines which affected cell should be processed first. Such a layer can potentially be coupled with more sophisticated compensation mechanisms or predictive controllers. This positioning is consistent with recent work on coordinated self-healing and zero-touch network management, while remaining computationally simple and explainable (Bayazeed et al., 2024; El Rajab et al., 2024).

An important finding is that PRS did not outperform conventional recovery on final recovery rate, recovery cycles, transferred users, maximum utilization, or final risk in the tested scenarios. The contribution demonstrated by the current model is therefore priority ordering, not superior final recovery efficiency. This is a meaningful result because the proposed mechanism changes the decision logic without changing the underlying recovery capacity. In an operational network, the benefit of improved ordering may become more visible when recovery resources are limited, when several cells compete for the same neighbor capacity, or when recovery actions have different costs. These conditions were not fully represented in the current simulation.

The V8 correction also highlights the importance of state consistency in self-healing simulations. A recovery algorithm must conserve the total number of users when users are transferred from one cell to another. Without source subtraction, the model artificially creates users and can produce misleading risk trends. The corrected model restored this conservation property and yielded consistent final results. This debugging stage strengthens the methodological validity of the proof of concept, although it does not replace validation against an operational network.

The main limitation is data availability. The final secondary dataset contains RSRP, RSRQ, and SNR but not throughput, latency, jitter, or packet loss. Consequently, Qi represents radio-quality degradation and not complete end-user QoS. The 69.47% Internet-access factor is a population proxy, not active LTE-user or operator traffic data. The 4,000-user cell capacity, traffic-surge factors, transfer limit, and neighbor relationships are simulation assumptions. No post-recovery field measurement was performed. These limitations mean that the study should be interpreted as a proof of concept. Recent research using live-network data demonstrates the additional value of richer operational KPIs and automated failure labeling, which should be incorporated in future validation (Sangaiah et al., 2022; Mata et al., 2024; Caleb et al., 2025).

This is an Creative Commons License This work is licensed under a Creative Commons Attribution-NonCommercial 4.0 International License.

Brilliance
Research of Artificial Intelligence

E-ISSN : 2807-9035
Volume 6, **Number** 4, November 2026
https://doi.org/10.47709/brilliance.v6i4.9992

CONCLUSION

This study developed a location-aware priority mechanism for LTE self-healing by integrating User Density Index, Traffic Load Index, and QoS Degradation Index. Across eight observation locations in Lhokseumawe, density ranged from 672 to 8,700 inhabitants/km², while the radio-based degradation index ranged from 0.026 to 0.908. The AHP configuration produced weights of 0.1638, 0.2973, and 0.5390 for user density, traffic load, and QoS degradation, with a consistency ratio of 0.79%. The resulting PRS ranked Alue Awe highest at 0.624 and Kuta Blang second at 0.608.

The results answer the first research question by showing that network condition is multidimensional: population concentration, estimated traffic demand, and radio quality do not follow a simple one-to-one relationship. The second research question is answered through the PRS-based model, which uses the three indicators to determine the order of recovery actions. After correction of source-destination accounting, the model achieved zero remaining overload and 100% simulated recovery in three multi-cell scenarios. However, PRS did not improve the final recovery rate or final risk compared with conventional recovery in the tested scenarios; its demonstrated contribution is the recovery-priority ordering.

The model is therefore a proof of concept rather than evidence of improved real-world LTE QoS. Future validation should integrate operator traffic counters and active-user data, direct end-user QoS measurements, and a larger set of cells and fault conditions. The AHP weights should also be replaced or calibrated using expert or operational evidence before deployment.

ACKNOWLEDGMENT

The authors acknowledge the financial support of Universitas Malikussaleh through the 2026 PNBP Research Development Scheme (Penelitian Pembinaan). The authors also acknowledge the research team members who contributed to data preparation, spatial processing, simulation development, and validation.

REFERENCES

Bayazeed, A., Khorzom, K., & Aljnidi, M. (2024). Towards coordinating self-healing instances: Policy-based and non-cooperative game theory-based approaches with location awareness. Computer Networks, 254, 110827. https://doi.org/10.1016/j.comnet.2024.110827

BPS-Statistics Lhokseumawe Municipality. (2024). Indikator kesejahteraan rakyat Kota Lhokseumawe 2024. Lhokseumawe, Indonesia: BPS-Statistics Lhokseumawe Municipality.

BPS-Statistics Lhokseumawe Municipality. (2025). Kota Lhokseumawe dalam angka 2025. Lhokseumawe, Indonesia: BPS-Statistics Lhokseumawe Municipality.

Caleb, S., Thangaraj, J. J. S., Padmapriya, G., Nandhini, T. J., Shadrach, F. D., & Latha, R. (2025). Revolutionizing fault detection in self-healing network via multi-serial cascaded and adaptive network. Knowledge-Based Systems, 309, 112732. https://doi.org/10.1016/j.knosys.2024.112732

El Rajab, M., Yang, L., & Shami, A. (2024). Zero-touch networks: Towards next-generation network automation. Computer Networks, 243, 110294. https://doi.org/10.1016/j.comnet.2024.110294

Gu, B., Zhan, J., Gong, S., Liu, W., Su, Z., & Guizani, M. (2023). A spatial-temporal transformer network for city-level cellular traffic analysis and prediction. IEEE Transactions on Wireless Communications, 22(12), 9412–9423. https://doi.org/10.1109/TWC.2023.3270441

Haider, U., Waqas, M., Hanif, M., Alasmary, H., & Qaisar, S. M. (2023). Network load prediction and anomaly detection using ensemble learning in 5G cellular networks. Computer Communications, 197, 141–150. https://doi.org/10.1016/j.comcom.2022.10.017

Li, S., Magli, E., Francini, G., & Ghinamo, G. (2024). Deep learning based prediction of traffic peaks in mobile networks. Computer Networks, 240, 110167. https://doi.org/10.1016/j.comnet.2023.110167

Mai, Y.-T., & Hu, C.-C. (2022). Design of dynamic resource allocation scheme for real-time traffic in the LTE network. EURASIP Journal on Wireless Communications and Networking, 2022, 14. https://doi.org/10.1186/s13638-022-02095-6

Mata, L., Sousa, M., Vieira, P., Queluz, M. P., & Rodrigues, A. (2024). On the use of spatial graphs for performance degradation root-cause analysis toward self-healing mobile networks. IEEE Access, 12, 20490–20508. https://doi.org/10.1109/ACCESS.2024.3361284

Nisa, F., & Haryadi, S. (2016). Simulation of the fault management with self healing mechanism (case study: LTE network in Banda Aceh area). In 2016 10th International Conference on Telecommunication Systems Services and Applications (TSSA) (pp. 1–6). IEEE. https://doi.org/10.1109/TSSA.2016.7871066

Omar, T., Ketseoglou, T., & Naffaa, I. (2021a). A novel self-healing model using precoding & big-data based approach for 5G networks. Pervasive and Mobile Computing, 73, 101365. https://doi.org/10.1016/j.pmcj.2021.101365

Omar, T., Ketseoglou, T., Naffaa, O., Marzvanyan, A., & Carr, C. (2021b). A precoding real-time buffer based self-healing solution for 5G networks. Journal of Computer and Communications, 9(6), 1–23. https://doi.org/10.4236/jcc.2021.96001

Ortega, A., & Tralli, V. (2022). QoS-aware resource allocation with pilot-aided channel estimation for heterogeneous

This is an Creative Commons License This work is licensed under a Creative Commons Attribution-NonCommercial 4.0 International License.

E-ISSN : 2807-9035
Volume 6, **Number** 4, November 2026
https://doi.org/10.47709/brilliance.v6i4.9992

wireless networks. Sensors, 22(12), 4545. https://doi.org/10.3390/s22124545

Oğuz, H. T., & Kalaycıoğlu, A. (2022). Anomaly detection in multi-tiered cellular networks using LSTM and 1D CNN. EURASIP Journal on Wireless Communications and Networking, 2022, 101. https://doi.org/10.1186/s13638-022-02183-7

Rao, Z., Xu, Y., Pan, S., Guo, J., Yan, Y., & Wang, Z. (2023). Cellular traffic prediction: A deep learning method considering dynamic nonlocal spatial correlation, self-attention, and correlation of spatiotemporal feature fusion. IEEE Transactions on Network and Service Management, 20(1), 426–440. https://doi.org/10.1109/TNSM.2022.3187251

Saaty, T. L. (2008). Decision making with the analytic hierarchy process. International Journal of Services Sciences, 1(1), 83–98. https://doi.org/10.1504/IJSSCI.2008.017590

Sangaiah, A. K., Rezaei, S., Javadpour, A., Miri, F., Zhang, W., & Wang, D. (2022). Automatic fault detection and diagnosis in cellular networks and beyond 5G: Intelligent network management. Algorithms, 15(11), 432. https://doi.org/10.3390/a15110432

Zaldivar-Herrera, J. E., Sánchez-Fernández, L. P., & Rodríguez-Méndez, L. M. (2024). Network Long-Term Evolution quality of service assessment using a weighted fuzzy inference system. Mathematics, 12(24), 3985. https://doi.org/10.3390/math12243985

Zhang, T., Zhu, K., & Hossain, E. (2022). Data-driven machine learning techniques for self-healing in cellular wireless networks: Challenges and solutions. Intelligent Computing, 2022, 9758169. https://doi.org/10.34133/2022/9758169

This is an Creative Commons License This work is licensed under a Creative Commons Attribution-NonCommercial 4.0 International License.